

ZnO nanowire network transistors based on a self-assembly method*

Dai Zhenqing(戴振清)^{1,2,†}, Chen Changxin(陈长鑫)¹, Zhang Yaozhong(张耀中)¹,
Wei Liangming(魏良明)¹, Zhang Jing(张竞)¹, Xu Dong(徐东)¹, and Zhang Yafei(张亚非)¹

¹Key Laboratory for Thin Film and Microfabrication of the Ministry of Education, Research Institute of Micro/Nano Science and Technology, Shanghai Jiao Tong University, Shanghai 200240, China

²Department of Physics and Chemistry, Hebei Normal University of Science and Technology, Qinhuangdao 066004, China

Abstract: Dense, uniform ZnO nanowire (NW) networks are prepared by using a simple and sufficient self-assembly method. In this method, ZnO NWs are modified with aminopropyltriethoxysilane (APTES) to form positively charged amine-terminated surfaces. The modified ZnO NWs are adsorbed on negatively charged SiO₂/Si substrates to form ZnO NW networks by the electrostatic interaction in an aqueous solution. Field-effect transistors (FETs) are fabricated and studied based on the ZnO NW networks. For a typical device with an NW density of 2.8 μm⁻², it exhibits a current on/off ratio of 2.4 × 10⁵, a transconductance of 336 nS, and a field-effect mobility of 27.4 cm²/(V·s).

Key words: self-assembly method; ZnO nanowire networks; field-effect transistors

DOI: 10.1088/1674-4926/33/8/084003

EEACC: 2550

1. Introduction

One-dimensional nanostructures such as nanowires (NWs) and nanotubes have attracted considerable interest for the fabrication of high-performance electronic and optical devices due to their excellent physical properties^[1–7]. Among them, ZnO NWs are one of the most important competitors, with their unique and diverse electrical, optic and piezoelectric properties. ZnO NWs are often used to fabricate field-effect transistors (FETs)^[8–10], gas sensors^[11], nanogenerators^[12], field emitters^[13, 14], light-emitting diodes^[15], and ultra violet (UV) detectors^[16].

Currently, most ZnO NW devices use single NWs^[8, 17–20]. A major drawback to these kinds of devices is the lack of a simple and sufficient process to precisely assemble single NWs, and the devices are prepared using a time-consuming process and one-by-one fabrication techniques. Therefore, large-scale fabrication of single NW devices is still a great challenge. Single NW devices are probably appropriate for fundamental research on the properties of devices and NWs, but not for practical application. ZnO NW networks have shown a promising future in the large-scale fabrication of devices with a relatively simple and low cost process, and also the devices based on them have advantages in large current output, high reliability, and reproducibility^[21, 22]. Comparing to well-aligned NW arrays, it is possible to have a contact resistance between the NWs for NW networks, but their process is simple and low cost^[23, 24].

Seung *et al.* reported a method for fabricating ZnO NW network FETs^[21]. In this method, NWs were synthesized by using a hydrothermal process on substrates where the devices were fabricated directly. The NWs in the networks were low crystalline and not horizontal, which degraded the performance

of device. Unalan *et al.* demonstrated another method in which the ZnO NWs and the networks were separate. The NWs were transferred from the growth substrate to the receiving one used for fabricating devices by using a contact printing process^[22]. This method provided the opportunity to fabricate NW network FETs with highly crystalline NWs, and the NWs on the receiving substrates were horizontal. However, the contact printing process had some difficulties in operation. For example, a very uniform pressure must be applied on the growth substrate, and the growth substrate must be lifted without any shear at the end. In addition, the NWs had to grow on a substrate in order to obtain the NW networks in the second method.

In this paper, we report our recent advance in the fabrication of ZnO NW networks. Highly dense, uniform ZnO nanowire networks are obtained by using a simple and sufficient self-assembly method. In this method, the surfaces of ZnO NWs are modified with aminopropyltriethoxysilane (APTES), which leads to the formation of an amine-terminated layer on the NWs. In aqueous solution, the modified NWs are adsorbed on negatively charged SiO₂/Si substrates depending on the electrostatic interaction due to the positively charged amine-terminated layer. This method provides the opportunity to fabricate network devices with highly crystalline NWs. And, most importantly, the NWs need not grow on a substrate in this method. In order to investigate the potential application of the prepared NW networks in devices, NW network FETs are fabricated.

2. Experimental details

ZnO NWs were synthesized by using a carbothermal reduction method without any catalyst^[25]. A quartz tube furnace was heated to 1100 °C, and then a mixed gas of air (0.1 L/min)

* Project supported by the National Science Foundation of China (Nos. 50730008, 60807008) and the Doctoral Fund of Hebei Normal University of Science and Technology (No. 2009YB007).

† Corresponding author. Email: daizhenqing@126.com

Received 11 May 2012, revised manuscript received 2 June 2012

© 2012 Chinese Institute of Electronics

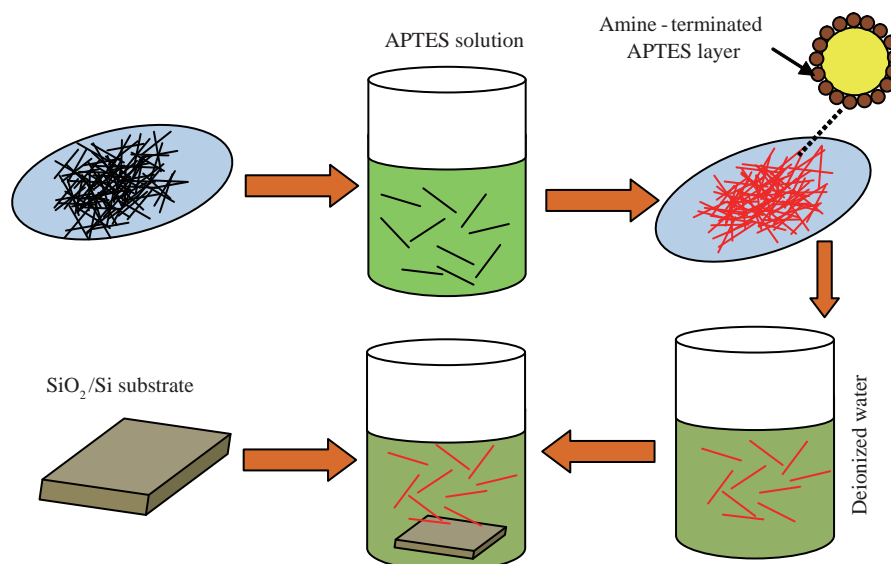


Fig. 1. Schematic diagram of the ZnO NW network deposition process.

and N_2 (4.5 L/min) was sent into the furnace. After 5 min, a quartz boat containing a mixture of ZnO powder (0.5 g) and graphite powder (0.5 g) was transferred to the furnace. Almost at the same time, the growth of ZnO NWs was initiated.

The SiO_2/Si substrates were ultrasonically rinsed with acetone, ethanol, and deionized water for 10 min in turn, and then were immersed in piranha solution (98wt% H_2SO_4 : 30wt% $H_2O_2 = 7 : 3$) for 2 h at 90 °C to make their surface hydrophilic. The APTES aqueous solution (0.5 mL APTES : 50 mL deionized water) was adjusted to the PH of 6.0 with HNO_3 , and then 50 mg of ZnO NWs were immersed in the solution and ultrasonically dispersed for 3 h. The suspension of NWs was centrifuged (12000 rpm, 25 min) five times to remove unwanted APTES. The modified NWs extracted from the suspension were ultrasonically dispersed in deionized water for 2 h followed by putting the pretreated substrates into the suspension of NWs. After a preset time, the substrates were taken out from the suspension, and then they were rinsed with deionized water several times in order to remove the loose NWs. Lastly, the ZnO NW networks on the substrates were annealed at 60 °C for 0.5 h. Figure 1 shows the schematic diagram depicting the method for the fabrication of NW networks.

FETs were fabricated with the ZnO NW networks by using a conventional photolithographic and lift-off process. On the top of the NW networks on the SiO_2/Si substrates, Ti/Au (40 nm/120 nm) source and drain electrodes were sputtered, with a defined channel width of 100 μm . The FETs were annealed at 200 °C for 1 h to make the APTES decompose. The devices were measured with an Agilent 4156C precision semiconductor parameter analyzer.

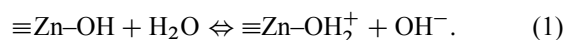
3. Results and discussion

3.1. ZnO NW networks

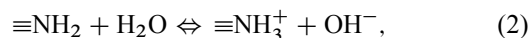
Figure 2(a) shows an SEM image of the synthesized NWs. The SEM image shows that some of NWs are branched. The average length and diameter of the synthesized ZnO NWs are about 1.7 μm and 34 nm, respectively. Figure 2(b) shows a

XRD pattern of synthesized ZnO NWs. The XRD pattern suggests that the ZnO NWs have the preferred orientation of (100). Figure 2(c) shows UV-vis absorption spectra of the synthesized ZnO NWs. The ZnO NWs have an absorbance peak at 370 nm corresponding to a band gap of 3.35 eV.

In aqueous solution, the surfaces of the ZnO NWs are hydrolysed and a layer of zinc hydroxides ($\equiv Zn-OH$) is formed. The hydroxide surfaces can become charged by reacting with H^+ or OH^- ions due to surface amphoteric reactions depending on the isoelectric point (IEP) of ZnO. The IEP of zinc oxide found in the literature ranges from 8.7 to 10.3^[26]. Below the IEP, hydroxide surfaces adsorb protons to produce positively charged surfaces^[27, 28]



For APTES, the amine group ($\equiv NH_2$) forms an amine salt [NH_3^+ , Eq. (2)] at pH = 2, while at pH = 12 the amine group is essentially free of hydrogen bonding. Between these two pH values, equilibrium is present. In all cases of pH ranges in aqueous solution, amino silanes hydrolyze into silanol ($\equiv Si-OH$), and the silanol group appears to be negatively charged due to lost protons [$\equiv Si-O^-$, Eq. (3)] at pH > 3^[28].



Based on the above discussion, at pH = 6, the surfaces of ZnO NWs should be positively charged, while for APTES the silanol group appears to be negatively charged. So, APTES is adsorbed on the surfaces of NWs depending on an electrostatic force of attraction, which leads to the formation of an amine-terminated layer on the surfaces of the NWs.

At pH = 7, the surfaces of the SiO_2/Si substrates are negatively charged due to the silanol losing protons, and the amine-terminated layers on the surfaces of the ZnO NWs are positively charged because of adsorbing protons of the amine group. So, the NWs modified with APTES are adsorbed on the SiO_2/Si substrates in aqueous solution.

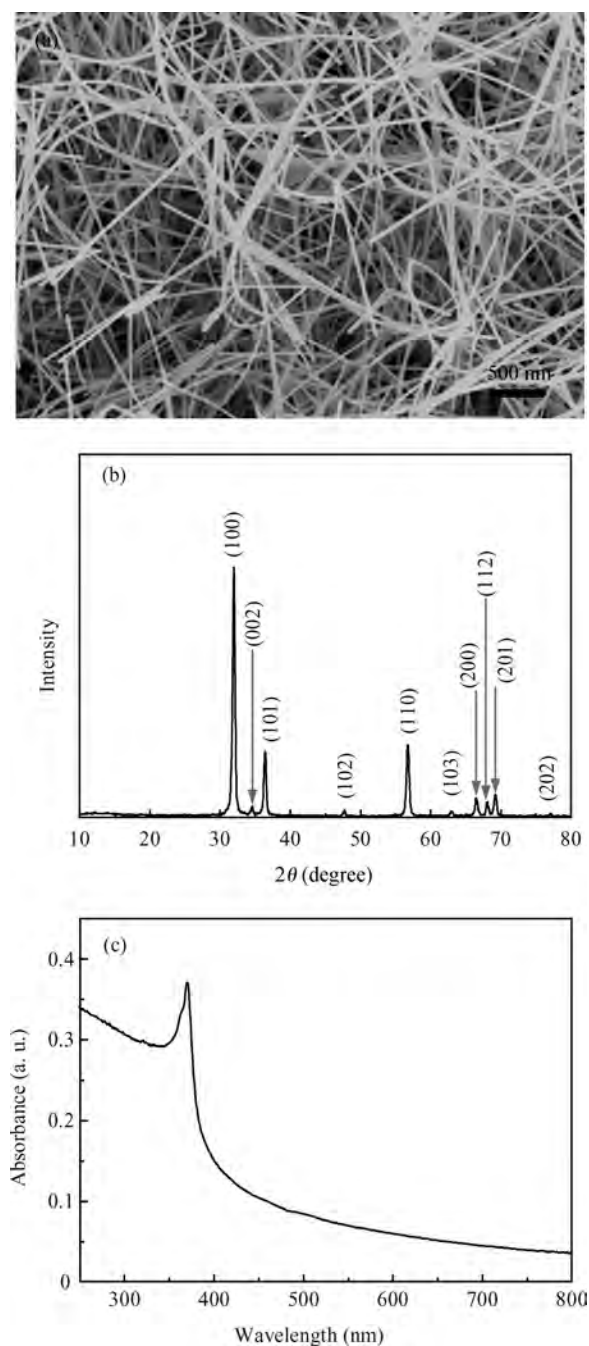


Fig. 2. (a) SEM image, (b) XRD pattern and (c) UV-vis absorption spectrum of synthesized ZnO NWs.

SEM images of the ZnO NW networks on the substrates with area of $2 \times 2 \text{ cm}^2$ immersed in the suspension of NWs are shown in Fig. 3. The SEM images show the deposited NWs at a randomly selected area on the corresponding substrates. The NW networks shown in Figs. 3(a)–3(d) correspond to the deposited time of 1 h, 1.5 h, 2 h, and 12 h, respectively. We find that the densities of NWs gradually increase with the deposited time extended and that they can be easily controlled by changing the deposition time. Highly dense, uniform NWs networks are prepared, and the density of NWs is $19 \mu\text{m}^{-2}$ for the network in Fig. 3(d).

In this method, NWs and networks are prepared separately, which gives the opportunity to fabricate network FETs with

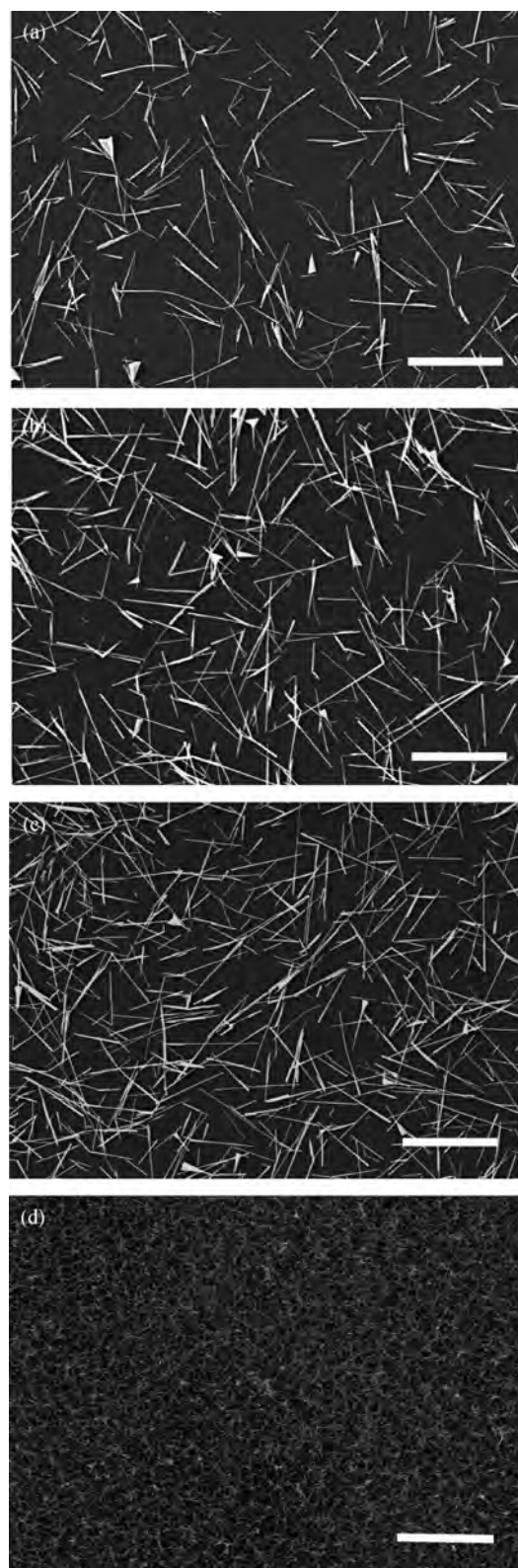


Fig. 3. SEM images of the ZnO NW network for different deposition times of (a) 1 h, (b) 1.5 h, (c) 2 h, and (d) 12 h. The scale bars are $5 \mu\text{m}$.

highly crystalline NWs. Furthermore, the NWs need not grow on a substrate in this method, which provides much more flexibility in the selection of NWs fabricated by different processes. The process is simple to operate, and there are no complicated

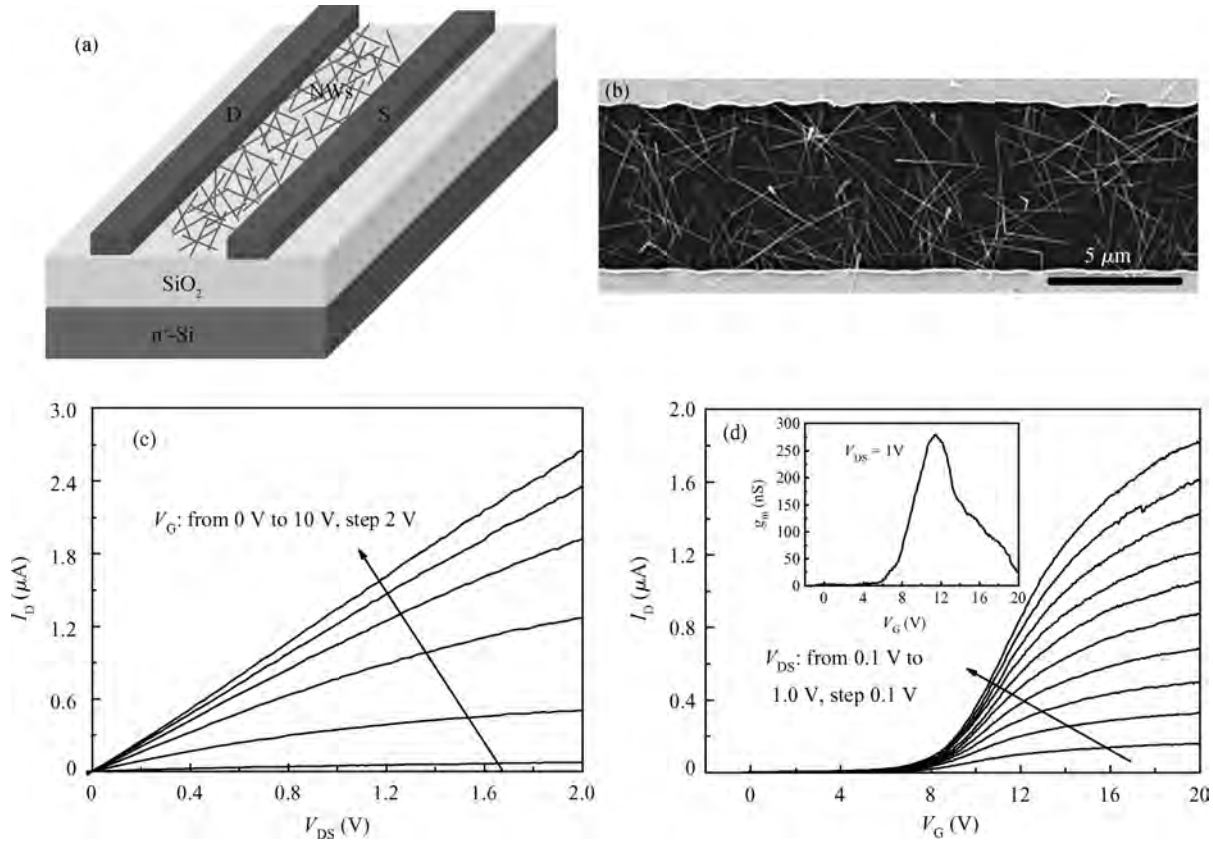


Fig. 4. (a) Schematic diagram of a ZnO NW network FET. (b) SEM image of a ZnO NW network FET with the NW density of $1.3 \mu\text{m}^{-2}$. (c) Output characteristic curves and (d) transfer characteristic curves of the ZnO NW network FET. Inset in (d) is the transconductance curve of the device.

steps. Most importantly, it is a low cost method. Therefore, the method is very appropriate for large-scale device fabrication.

3.2. ZnO NW network FETs

The schematic diagram of a ZnO NW network FET is shown in Fig. 4(a). Heavily doped n-type silicon is used as the back gate and SiO₂ (500 nm) is used as the back-gate dielectric. S and D are the source and drain electrodes. The devices annealed at 200 °C were placed in ambient conditions for three days before they are measured. A SEM image of a device is shown in Fig. 4(b), and the NW density is $1.3 \mu\text{m}^{-2}$. Figure 4(c) shows the output characteristics of the device at different gate voltages V_G , and Figure 4(d) shows its transfer characteristics at different drain–source voltages V_{DS} . The inset in Fig. 4(d) is the transconductance of the device at $V_{DS} = 1$ V. From the output characteristics, we learn that the NWs exhibit an n-type semiconductive property, which is attributed to the existing N₂ in the process of synthesizing NWs. The N₂ leads to the formation of a Zn₁–N₀ complex, which provides a donor level of 30 meV under the conduction band edge^[29]. The output characteristic curves are almost linear, which shows the contacts between NWs and Ti/Au electrodes are ohmic. From the transfer characteristic curves, the current on/off ratio is estimated to be 1.0×10^6 , which is comparable to the one reported in Refs. [21, 22, 30]. In addition, the threshold voltage is estimated to be 9.1 V. The maximum transconductance is estimated to be 278 nS which is higher than that in Ref. [21]. The field-effect mobility can be calculated from the equation

$$\mu_{fe} = \frac{g_m L}{WC_{ox} V_{DS}}, \quad (4)$$

in the linear operation regime. Here L ($6.4 \mu\text{m}$) and W are the device channel length and width, $g_m = dI_D/dV_G$ is the linear-region transconductance, and C_{ox} is the gate capacitance per unit area which can be obtained from a parallel plate model

$$C_{ox} = \varepsilon_0 \varepsilon_r / t_{ox}, \quad (5)$$

where ε_0 is the vacuum dielectric constant, ε_r is the average relative dielectric constant of SiO₂ (3.9) and air (1), and t_{ox} is the thickness of SiO₂ layer. The mobility is estimated to be $4.1 \text{ cm}^2/(\text{V}\cdot\text{s})$, which is higher than that in Refs. [21, 30].

For the device, the sparse NWs lead to the low coverage of SiO₂ layer. Thus, the mobility is underestimated when the original channel width is used in Eq. (4). An effective channel width substituting for the original one can be used in mobility calculations. The effective channel width was estimated as the product of the average of the NW diameter and the number of NWs on the source and drain contacts^[22]. With the effective channel width, the mobility is estimated to be $30.5 \text{ cm}^2/(\text{V}\cdot\text{s})$, which is comparable to the one in Ref. [22]. In the following discussion, we will focus on a device with a higher NW density of $2.8 \mu\text{m}^{-2}$. An SEM image of the device is shown in Fig. 5(a), and its channel length is $8.5 \mu\text{m}$. Transfer characteristics of the device are shown in Fig. 5(b). The inset in Fig. 5(b) is the transconductance of the device. The mobility is estimated to

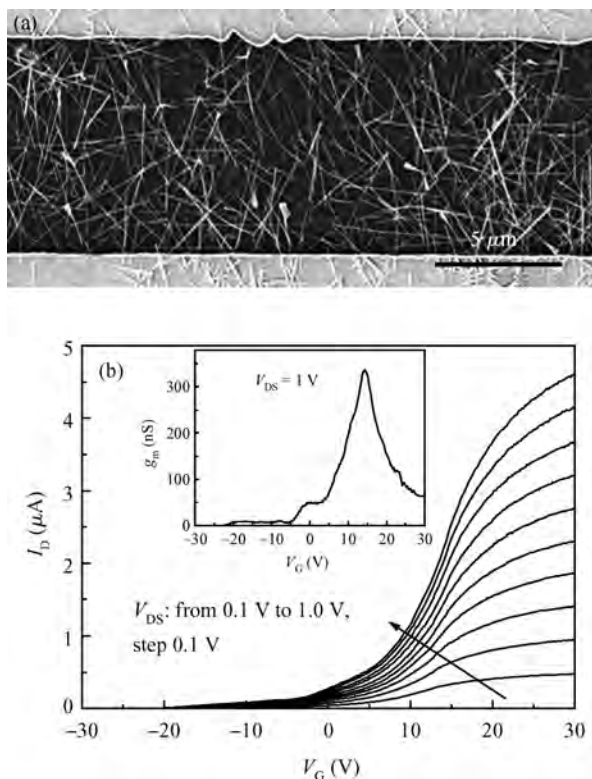


Fig. 5. (a) SEM image of a ZnO NW network FET with the NW density of $2.8 \mu\text{m}^{-2}$. (b) Transfer characteristic curves of a ZnO NW network FET with the NW density of $2.8 \mu\text{m}^{-2}$. Inset in (b) is the transconductance curve of the device.

be $27.4 \text{ cm}^2/(\text{V}\cdot\text{s})$ with the effective channel width. The maximum transconductance is estimated to be 336 nS , the on/off ratio is estimated to be 2.4×10^5 , and the threshold voltage is 8.1 V for the device.

4. Conclusion

In summary, we have successfully prepared highly dense, uniform ZnO NW networks by using a simple and sufficient method, and the NW density can be easily controlled by changing the deposition time. In this method, the NWs are modified with APTES, and an amine-terminated layer is formed on the surfaces of the modified NWs. In aqueous solution, the modified NWs with the positively charged amine-terminated layer will adsorb on the negatively charged SiO_2/Si substrates. For an FET based on the fabricated NW networks with the NW density of $2.8 \mu\text{m}^{-2}$, the field-effect mobility is estimated to be $27.4 \text{ cm}^2/(\text{V}\cdot\text{s})$, the transconductance is estimated to be 336 nS , and the on/off ratio is estimated to be 2.4×10^5 . The proposed method gives an opportunity to fabricate ZnO NW devices on a large-scale by a simple and low cost process.

References

- [1] Yan H, Choe H S, Nam S W, et al. Programmable nanowire circuits for nanoprocessors. *Nature*, 2011, 470(7333): 240
- [2] Huang M H, Mao S, Feick H, et al. Room-temperature ultraviolet nanowire nanolasers. *Science*, 2001, 292(5523): 1897
- [3] Chen C X, Lu Y, Kong E S, et al. Nanowelded carbon-nanotube-based solar microcells. *Small*, 2008, 4(9): 1313
- [4] Chen C X, Yan L J, Kong E S, et al. Ultrasonic nanowelding of carbon nanotubes to metal electrodes. *Nanotechnology*, 2006, 17(9): 2192
- [5] Chen C X, Zhang W, Kong E S, et al. Carbon nanotube photo-voltaic device with asymmetrical contacts. *Appl Phys Lett*, 2009, 94(26): 263501
- [6] Chang P, Liu S, Chen R B, et al. Low temperature synthesis and optical properties of ZnO nanowires. *Chinese Journal of Semiconductors*, 2007, 28 (10): 1503
- [7] Lang J H, Yang J H, Li C S, et al. Photoluminescence properties of ZnO nanorods prepared under low temperature. *Journal of Semiconductors*, 2008, 29(11): 2260
- [8] Goldberger J, Sirbuly D J, Law M, et al. ZnO nanowire transistors. *J Phys Chem B*, 2005, 109(1): 9
- [9] Ju S Y, Lee K H, Yoon M H, et al. High performance ZnO nanowire field effect transistors with organic gate nanodielectrics: effects of metal contacts and ozone treatment. *Nanotechnology*, 2007, 18(15): 155201
- [10] Fu X J, Zhang H Y, Guo C X, et al. Fabrication and photoelectrical characteristics of ZnO nanowire field-effect transistors. *Journal of Semiconductors*, 2009, 30(8): 084002
- [11] Ahn M W, Park K S, Heo J H. Gas sensing properties of defect-controlled ZnO-nanowire gas sensor. *Appl Phys Lett*, 2008, 93(26): 263103
- [12] Wang X D, Song J H, Liu J, et al. Direct-current nanogenerator driven by ultrasonic waves. *Science*, 2007, 316(5821): 102
- [13] Huang Y H, Zhang Y, Gu Y S, et al. Field Emission of a single In-doped ZnO nanowire. *J Phys Chem C*, 2007, 111(26): 9039
- [14] Wang L J, Yang Z X, Lin J Y, et al. Influence of morphologies on the field emission performance of oriented ZnO nano-arrays. *Journal of Semiconductors*, 2011, 32(12): 123001
- [15] Bao J M, Zimmler M A, Capasso F, et al. Broadband ZnO single-nanowire light-emitting diode. *Nano Lett*, 2006, 6(8): 1719
- [16] Kind H, Yan H Q, Messer B, et al. Nanowire ultraviolet photodetectors and optical switches. *Adv Mater*, 2002, 14(2): 158
- [17] Park W, Hong W K, Jo G, et al. Tuning of operation mode of ZnO nanowire field effect transistors by solvent-driven surface treatment. *Nanotechnology*, 2009, 20(47): 475702
- [18] Sohn J I, Choi S S, Morris S M, et al. Novel nonvolatile memory with multibit storage based on a ZnO nanowire transistor. *Nano Lett*, 2010, 10(11): 4316
- [19] Choi A, Kim K, Jung H, et al. ZnO nanowire biosensors for detection of biomolecular interactions in enhancement mode. *Sens Actuators B*, 2010, 148(2): 577
- [20] Kim K, Debnath P C, Kim S, et al. Temperature stress on pristine ZnO nanowire field effect transistor. *Appl Phys Lett*, 2011, 98(11): 113109
- [21] Ko S H, Park I, Pan H, et al. ZnO nanowire network transistor fabrication on a polymer substrates by low-temperature, all-inorganic nanoparticle solution process. *Appl Phys Lett*, 2008, 92(15): 154102
- [22] Unalan H E, Zhang Y, Hiralal P, et al. Zinc oxide nanowire networks for macroelectronics devices. *Appl Phys Lett*, 2009, 94(16): 163501
- [23] Wang C, Zhang J L, Ryu K, et al. Wafer-scale fabrication of separated carbon nanotube thin-film transistors for display applications. *Nano Lett*, 2009, 9(12): 4285
- [24] Sun D M, Timmermans M Y, Tian Y, et al. Flexible high-performance carbon nanotube integrated circuits. *Nature Nanotech*, 2011, 6(3): 156
- [25] Zhou Z H, Zhan C H, Wang Y Y, et al. Rapid mass production of ZnO nanowires by a modified carbothermal reduction method.

- Mater Lett, 2011, 65(5): 832
- [26] Parks G A. The isoelectric points of solid oxide, solid hydroxides, and aqueous hydroxocomplex systems. Chem Rev, 1965, 65(2): 177
- [27] Degen A, Kosec M. Effect of pH and impurities on the surface charge of zinc oxide in aqueous solution. J Eur Ceram Soc, 2000, 20: 667
- [28] Grasset F, Saito N, Li D, et al. Surface modification of zinc oxide nanoparticles by aminopropyltriethoxysilane. J Alloys Compd, 2003, 360(1/2): 298
- [29] Look D C, Farlow G C, Reunchan P, et al. Evidence for native-defect donors in n-type ZnO. Phys Rev Lett, 2005, 95(22): 225502
- [30] Sun B Q, Sirringhaus H. Solution-processed zinc oxide field-effect transistors based on self-assembly of colloidal nanorods. Nano Lett, 2005, 5(12): 2408